

Involvement of moesin phosphorylation in ischemia/reperfusion induced inner blood-retinal barrier dysfunction

Jing Xu¹, Qiong Liu¹, Ming Ma¹, Lin-Jiang Chen¹, Jian Yu¹, Ke Xiong¹, Jing Wu²

¹Department of Ophthalmology, Nanfang Hospital, Southern Medical University, Guangzhou 510515, Guangdong Province, China

²Huiqiao Medical Center, Nanfang Hospital, Southern Medical University, Guangzhou 510515, Guangdong Province, China

Correspondence to: Jing Wu. Huiqiao Medical Center, Nanfang Hospital, Southern Medical University, Guangzhou 510515, Guangdong Province, China. wujingsci@126.com

Received: 2019-08-29 Accepted: 2020-02-12

Abstract

• **AIM:** To investigate the role of moesin and its underlying signal transduction in retinal vascular damage induced by retinal ischemia-reperfusion (RIR) insult.

• **METHODS:** C57BL/6 mice were subjected to continued ischemia for 45min, followed by blood reperfusion. The expression and phosphorylation of moesin in retinal vessels were detected by immunohistochemistry and Western blotting. The inner blood-retinal barrier was evaluated using FITC-dextran leakage assay on whole-mount retina. Further studies were conducted to explore the effects of p38 mitogen-activated protein kinase (MAPK) pathway on the involvement of moesin in RIR-evoked retinal vascular hyperpermeability response.

• **RESULTS:** It revealed that RIR induced moesin phosphorylation in a time-dependent manner after reperfusion. The phosphorylation of moesin was alleviated by inhibitions of p38 MAPK, while this treatment also ameliorated the dysfunction of inner blood-retinal barrier.

• **CONCLUSION:** The results suggest that moesin is involved in RIR-evoked retinal vascular endothelial dysfunction and the phosphorylation of moesin is triggered via p38 MAPK activation.

• **KEYWORDS:** retinal ischemia-reperfusion; moesin; p38 mitogen-activated protein kinase; inner blood-retinal barrier; mice

DOI:10.18240/ijo.2020.04.03

Citation: Xu J, Liu Q, Ma M, Chen LJ, Yu J, Xiong K, Wu J. Involvement of moesin phosphorylation in ischemia/reperfusion induced inner blood-retinal barrier dysfunction. *Int J Ophthalmol* 2020;13(4):545-551

INTRODUCTION

Retinal ischemia/reperfusion (RIR) injury contributes to visual impairment even blindness in several ocular diseases, like glaucoma, retinal vascular occlusions, diabetic retinopathy and ischemic optic neuropathy for instance, causing damage to the whole retina^[1]. Decreased blood flow (ischemia) in the retinal vasculature gives rise to a state of retinal hypersensitivity to nutrients and oxygen, exacerbating serious inflammatory, excitatory toxicity and oxidative stress when blood flow is subsequently returned (reperfusion)^[2]. Current therapeutic treatments for retina RIR injury focus on recovering retinal blood supply through laser, vasodilators, and anticoagulants, or mitigating oxidative stress by free radical scavengers^[3]. A mouse model of acute elevation of intraocular pressure (IOP) followed by reperfusion have begun to elaborate the mechanisms underlying RIR-triggered retinal neurovascular damage^[4].

Vascular dysfunction is central to RIR injury, understanding the precise mechanisms in RIR-mediated retina vascular disease is essential. Retinal transient ischemia may result in a breakdown of the inner blood-retinal barrier, which is featured by the tight junctions between neighboring retinal capillary endothelial cells (ECs), disruption of the EC barrier associates with vascular hyperpermeability and leakage of albumin and fluid, leading to tissue edema with consequent retina function impairment^[5]. Ezrin-radixin-moesin (ERM) proteins are supposed as cross linkers between actin filaments and the plasma membrane, engaging in cell adhesion, morphology, motility, mitosis, and cell polarity^[6]. Moesin is the main member of ERM family expressed by endothelium^[7], it was demonstrated to have a pivotal role in advanced glycation end products (AGEs)-evoked cytoskeleton reorganization and endothelial barrier dysfunction in human dermal microvascular endothelial cells (HMVECs)^[8-9], knockdown of moesin expression with siRNA could compromise the F-actin stress fiber formation and the hyperpermeability response.

This study aims to clarify the role of moesin phosphorylation in the mouse retina after RIR injury, and to investigate the possible molecular signaling pathways activated in RIR induced inner blood-retinal barrier (iBRB) disruption.

MATERIALS AND METHODS

Ethical Approval Animals used in our experiments was in compliance with the ARVO Statement for the Use of Animals in Ophthalmic and Vision Research and executed with the consent of the Animal Care Committee of Southern Medical University.

Materials The 20-25 g male C57BL/6J mice were acquired from the Laboratory Animal Center of Southern Medical University. Mice were housed under standard conditions of temperature and humidity, with a 12h light and dark cycle and free access to food and water. Antibodies against total moesin and phospho-moesin (Thr558), were purchased from Abcam (Cambridge, UK). Antibodies against total and phospho-p38 mitogen-activated protein kinase (MAPK), FITC-conjugated neuronal nuclei (NeuN) were purchased from Cell Signaling Technology (Boston, USA). p38 inhibitor SB203580 were acquired from Selleck Chemicals (Houston, USA). FITC-dextran and other reagents were purchased from Sigma-Aldrich (St. Louis, MO, USA) unless otherwise indicated.

Transient Retinal Ischemia A total of 65 mice were used in our study and randomly divided into different groups, according to experimental requirement respectively. The animals were anesthetized by injection of 3% pentobarbital sodium (50 mg/kg, Sangon Biotech, Shanghai, China) intraperitoneally, pupils were dilated with 1% tropicamide (Santen Pharmaceutical, Osaka, Japan). The 0.4% oxybuprocaine hydrochloride eye drops (Santen Pharmaceutical, Osaka, Japan) was used as topical anesthesia to alleviate the discomfort of the animals. Retinal ischemia was conducted by an acute increase of the IOP, according to the method previously reported^[10-11]. A 33-gauge infusion needle (Hamilton, Switzerland), connected to a reservoir filling with normal saline (0.9% NaCl), was inserted in the anterior chamber of the left eye, and the saline container was risen to produce an IOP of 120 mm Hg for 45min. Ischemia was confirmed as the whitening of the conjunctiva and blocking of the retinal arteries observed by microscopic examination^[10-11]. Sham eyes were treated by briefly piercing a 33-gauge needle through the cornea, the needle connected with a same saline container, but without elevating the IOP. Ofloxacin eye ointment (Santen Pharmaceutical, Osaka, Japan) was applied to the cornea after needle removal.

Histopathology and Morphology of Retina After the mice were killed, eyeballs were enucleated at 1h and 7d respectively following RIR. The eyeballs were instantly fixed with eyeball fixation fluid (G1109, Servicebio), and then embedded in paraffin, 4 μ m paraffin sections were incised in the vertical meridian through the optic disc. The sections were stained with hematoxylin and eosin (HE), and retina images were then photographed using light microscope (Olympus BX51).

Retinal injury was assessed as reported in previous researches. Changes in the thickness of different retinal layers were analyzed with Image J in the same topographic region of each retina (1 mm from the optic nerve head), under 400 \times with an ocular micrometer.

Fluorescence Staining of Neurons in Ganglion Cell Layer

Eyeballs were removed upon euthanasia and incubated in 4% paraformaldehyde at room temperature. The retinas were separated after 1h strong fixation, then were cryoprotected in 30% sucrose overnight. The freeze-thaw cycle was requested for 3 times, which means cryoprotected retinas are frozen in liquid nitrogen and immediately unfrozen at room temperature. The retinas were then washed with 0.1 mol/L Tris buffer at least 3 times, blocked for 1h in buffer (5% bovine serum, 0.1% Triton X-100 in 0.1 mol/L Tris buffer) and incubated with FITC-conjugated neuronal nuclei antibody (1:500) at 4 $^{\circ}$ C overnight. After thoroughly washed using 0.1 mol/L Tris buffer, the retinas were then flat-mounted on a glass slide. Covered with a glass slip, NeuN positive neurons in the ganglion cell layer (GCL) were pictured under fluorescence microscope (Olympus BX63). NeuN-positive neurons were counted by Image J. This software measures cells semi-automatically, which means that it records the number of cells that are clicked on by the operator identifying cells in the image.

Western Blotting Protein extracted from retina were prepared and size-separated in sodium dodecyl sulfate polyacrylamide gel (SDS-PAGE), subsequently transferred to polyvinylidene difluoride (PVDF) membranes (Invitrogen). The membrane was blocked with 5% bovine serum albumin for 1h and incubated overnight at 4 $^{\circ}$ C with primary antibodies of moesin, phospho-moesin, p38 and phospho-p38 with 1:1000 dilution. Afterwards, they were incubated with respective second antibodies for 1h at room temperature. Signals were detected using chemiluminescence reagents. Quantification of the protein bands were conducted using the software Quantity One (Bio-Rad Laboratories, Hercules, CA, USA).

Immunohistochemical Staining Whole-mount of eyeball was enucleated upon euthanasia immediately, fixed with eyeball fixation fluid for 12-24h at room temperature, and then embedded in paraffin. Then, 4- μ m paraffin slides of the eyeball were incubated with primary antibody overnight, after deparaffinization and antigen retrieval. After being washed for 3 times, samples were incubated with secondary antibody at room temperature for 1h. Finally, samples were conducted with DAB substrate working solution and photographed with a light microscope (Olympus BX51).

Assessment of Blood-Retinal Inner Barrier Function Forty-five minutes after induction of transient retinal ischemia, the needle was removed to reperfuse the vessel. For p38 MAPK inhibitor treatment group, mice received a SB203580 (1 mg/kg)

injection intraperitoneally 30min before the RIR induction, then *in vivo* vascular permeability in the retina was measured. Mice were anesthetized before all surgical manipulations for the microvascular exudation assay using FITC-dextran. Briefly, the butterfly needle of the perfusion device was inserted into the mice left ventricle, followed by a puncture at the right atrium using a needle. Sequentially, 2 mL of PBS was injected from the perfusion device at the rate of 1-2 mL/min (total 1-2min), followed by injection of 5-10 mL FITC-dextran at the rate of 1-2 mL/min (total 10-15min). Monitor color change in the ears, nose and palms. Finally, the animal was perfused with 1% formaldehyde for fixation and enucleated. Retinas were separated from eyeball, and were dissected with four radial incisions and flat-mounted on glass slides with fluoromount mounting medium (Sigma-Aldrich, St.Louis, MO, USA). Images were captured under fluorescence microscope (Olympus BX63), for each retina, at least 5 different view fields were chosen to collect images. Integrated optical intensity changes were calculated using formula: $\Delta I = 1 - (I_i - I_o) / I_i$, where I_i is the light intensity inside the vessel, I_o is the light intensity outside the vessel, and ΔI indicates the changes in light intensity.

Statistical Analysis Data was displayed as the mean±SD from at least 3 independent experiments, and SPSS version 19.0 software (SPSS, Inc., Chicago, IL, USA) was used to analyze the data. One-way ANOVA was performed in statistical comparisons between groups, followed by Bonferroni post hoc test. $P < 0.05$ was considered a statistically significant difference.

RESULTS

Morphologic and Histologic Changes in Retina Following RIR As for the retina of sham mice, the whole retinal thickness was $156.89 \pm 1.18 \mu\text{m}$ at 1h and $174.98 \pm 5.24 \mu\text{m}$ at 7d, no significant difference was found between these two groups. One hour post-RIR, a significant increase in the thickness of the whole retina was detected, especially in the GCL and inner plexiform layer (IPL; retinal thickness: $228.49 \pm 34.23 \mu\text{m}$; GCL: $52.92 \pm 4.69 \mu\text{m}$; IPL: $93.27 \pm 17.91 \mu\text{m}$), indicating the swelling of retina subjected to RIR, which might be attributed to the vascular hyperpermeability and breakdown of the iBRB. However, a significant decrease in the thickness of the whole retina, GCL and IPL (retinal thickness: $57.11 \pm 5.12 \mu\text{m}$; GCL: $52.92 \pm 4.69 \mu\text{m}$; IPL: $5.17 \pm 0.79 \mu\text{m}$) was distinct in the eyes of RIR at 7d after RIR, suggesting an atrophy followed by the microvascular dysfunction (Figure 1A-1C). Furthermore, whole retina flat-mounts were stained for the neuronal marker NeuN to verify the number of surviving neurons in the GCL. The results showed that the density of FITC-labeled RGCs decreased visibly 7d post-RIR (Figure 1D, 1E), indicating the cumulative degeneration of neurons, in accordance with the previous views that RIR insult

could induce a cumulative damage to neurons which peaked at one week after reperfusion^[12].

Moesin Phosphorylation in Retina from RIR-treated Mice Since ERM proteins, especially moesin, has been reported that it can regulate endothelial permeability *via* maintaining ECs' equilibrium between contractile forces (CF) and adhesive forces (AF), CF was generated by the endothelial cytoskeleton, and AF was produced from the cell-matrix attachment and inter-endothelial junctions^[13], therefore here we asked whether RIR can evoke moesin phosphorylation. Western blot revealed a significant upregulation of moesin phosphorylation at threonine 558 residue, in the retinal lysates that obtained from RIR-treated mice (Figure 2A). Phosphorylation of moesin was immediately but slightly enhanced after ischemic insult, reached a peak at 1h after vessel reperfusion, and then decreased to a relatively stable level, as compared with the sham group, based on these results, we detected moesin expression at 1h after reperfusion in subsequent mechanistic experiments. No difference in total moesin expression was found between RIR conducted and sham groups.

Retina immunohistochemistry showed that moesin and phospho-moesin were only probed in inner retina microvessel's ECs, indicating the specific distribution of moesin in ECs (Figure 2D), which was consistent with previous theories that moesin is supposed to be the main ERM molecule expressed specifically by endothelium^[8]. In accordance with the result of Western blot, phospho-moesin was expressed prominently in the inner retina 1h after RIR.

Blocking the p38 MAPK Pathway Alleviated the RIR Triggered Moesin Activation Several previous researches have revealed that p38 MAPK played a pivotal role in AGEs-induced moesin phosphorylation in HMVECs^[8]. We asked whether p38 MAPK signaling act as a role in moesin activation in this retina RIR mice model. Demonstrated by the upregulated expression of phosphorylated p38 MAPK, we testified that p38 MAPK was effectively activated in retinal vasculature under RIR insult. While this activation was markedly reduced by treatment of specific p38 inhibitor (SB203580) 30min prior each RIR induction. Correspondingly, there was an obvious abatement in threonine 558 phosphorylation of moesin at the same time (Figure 3), indicating that p38 MAPK activation was involved in RIR-evoked moesin phosphorylation. Whereas total moesin protein expression remain stable during this process.

Suppression of the p38 MAPK Pathway Protects Retina from RIR Evoked Barrier Dysfunction Phospho-moesin is localized primarily at the ECs periphery without any stimulation, but treatment with AGEs induces an increased phospho-moesin density in the cytoplasm of ECs, and it is further polymerized to sarciniform fibers. Therefore, moesin is

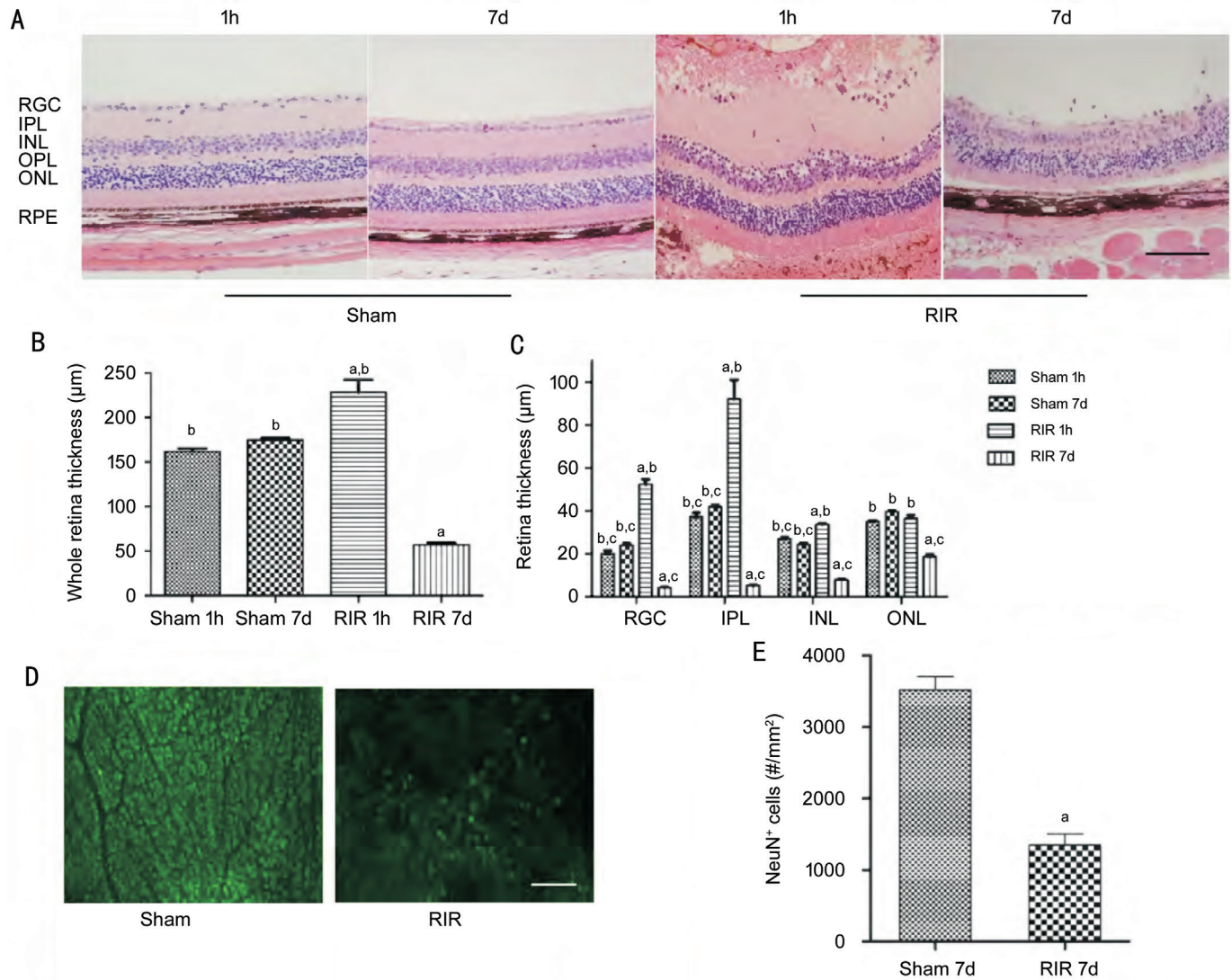


Figure 1 RIR related insults on retinal morphology and RGCs survival A: Photomicrographs of retina cross-sections from Sham and RIR treated eyes. Mean thickness in all layers of retina and separated RGC, IPL and INL layer showed a remarkable increase 1h following the RIR insult, while there was a significant decrease 7d after RIR. All micrographs were taken 1 mm from the optic nerve head, $n=3$. HE staining under $400\times$ magnification. B, C: Data represent mean thickness of whole retina and separate layers in all experimental groups (mean \pm SD; $^aP<0.05$ vs Sham 1h; $^bP<0.01$ vs RIR 7d; $^cP<0.01$ vs RIR 1h.). D: Representative fluorescent pictures of NeuN-positive GCLs (green) in flat-mounted retina 7d after reperfusion, showing as sham and RIR groups respectively. Progressive loss of NeuN-labeled RGCs population was observed 7d after injury, $n=5$. Fluorescence staining under $200\times$ magnification. Scale bar: 50 μ m. E: Bar graph showing significant decrease of NeuN⁺ RGCs in the RIR insulted eyes compared with sham eyes. $^aP<0.05$.

considered as a bridging molecule between actin cytoskeleton and plasma membrane^[8]. *In vivo*, images from microscopy demonstrated an obvious increase in dextran leakage outside the vessels in RIR-treated mice. On the contrary, the mice in sham group showed little extravasation of dextran, suggesting the microvascular hyperpermeability induced by RIR. However, pretreatment of SB203580 1h before RIR could significantly attenuate the leakage (Figure 4).

DISCUSSION

Ischemia reperfusion injury is a complicated and systemic pathophysiological process, it is initiated by the obstruction of blood flow to tissue and consequent ischemia, subsequently followed by the reperfusion of circulation. RIR injury

precipitates various cellular damages in several ocular diseases, such as oxidative stress and downstream inflammatory cascade^[14]. To some degree, the development of RIR injury is attributed to microvascular barrier dysfunction and hemodynamic alternations^[15]. Disruption of vascular endothelial integrity leads to capillary hyperpermeability and extravasation of fluid^[16]. Nevertheless, the precise mechanism underlying ECs dysfunction induced by RIR remains ambiguous. Hereby, in our present study, we demonstrated that under RIR insult, moesin phosphorylation at threonine 558 was dramatically enhanced in retinal endothelium, and the upregulation of moesin phosphorylation could be alleviated by suppression of p38 MAPK activation. RIR injury contributed

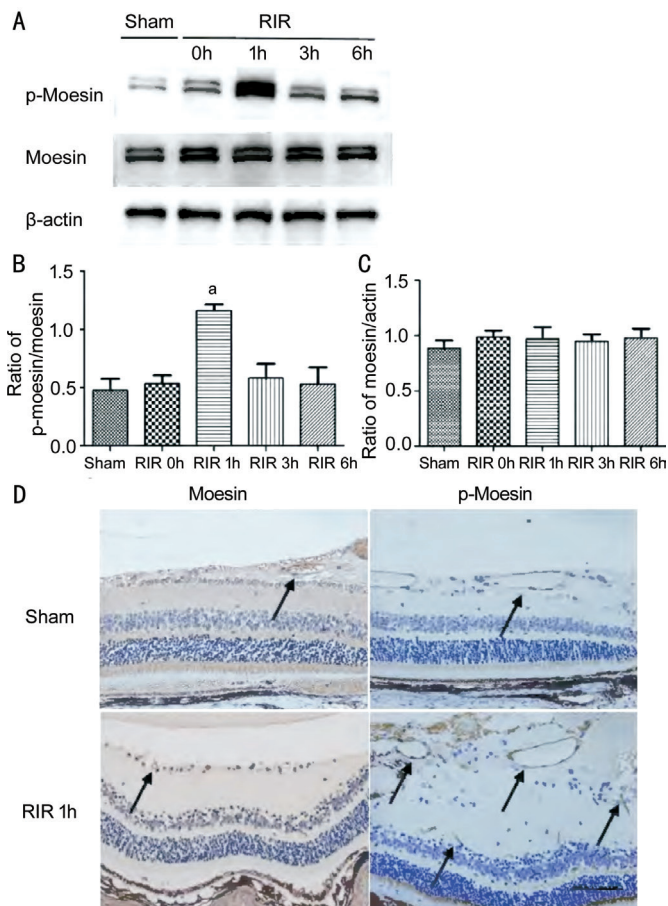


Figure 2 RIR triggered time-dependent phosphorylation of moesin in retina tissue A: The retinal lysates from sham group and 0, 1, 3, 6h after reperfusion were prepared and detected using Western blot analysis, with antibodies against moesin and the phospho-moesin. B: Moesin phosphorylation was presented as the ratio of total moesin in the same group. C: Total moesin expression was presented as the ratio of β -actin. $n=5$, $^aP<0.05$. D: Immunohistochemical staining of paraffin-embedded mouse retina was performed, with indicated antibodies. Expression of protein was visualized using a diaminobenzidine reagent (brown, as arrows indicated). Moesin was stained predominantly in endothelium of retinal micro-vasculature. The expression of phospho-moesin was increased remarkably in RIR-treated retina, $n=3$. Immunohistochemical staining under 400 \times . Scale bar: 50 μ m.

to the destruction of iBRB integrity, causing retinal vascular hyperpermeability and tissue edema, however, inhibition of p38 MAPK activation prevented these RIR-triggered alterations.

We used a pressure-induced retinal RIR injury to model this pathology, in this model, blood supply from both the retinal and choroidal circulation is obstructed instantly by increasing the IOP up to 120 mm Hg, and reinstated by the removal of the needle^[16]. Our study showed that RIR related insults caused a marked thickening in the whole retinal thickness and diffused tissues edema 1h after reperfusion, especially the inner retina including RGC, IPL, INL layers. Subsequently, 7d after RIR,

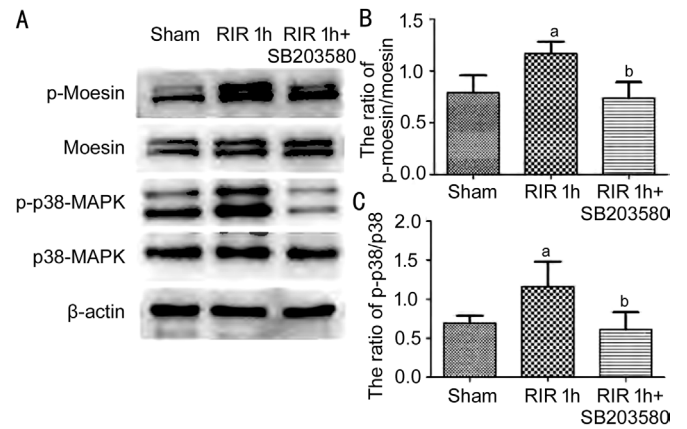


Figure 3 P38 inhibition with SB203580 attenuate moesin phosphorylation in retinal tissue A: Mice were treated with or without SB203580 for 30min before RIR execution, Western blotting of indicated proteins were measured and shown in the image. B, C: P38 or moesin phosphorylation was presented as the ratio of total p38 or moesin in the same group. $n=5$. $^bP<0.05$ vs RIR, $^aP<0.05$ vs control.

decreased thickness, extensive disorganization of the retinal histoarchitecture, as well as an overt reduction in the loss of RGCs were displayed.

As associated with vasogenic leakage and oedema, free radical production, disruption of ionic homeostasis, and energy failure during RIR are also considerable factors facilitating the swollen of neurocytes, like astrocytes^[5], which spanned in the entire thickness of inner retina^[17]. Aberrant activations of astrocytes and Müller cells were implicated by the upregulation of glial fibrillary acidic protein (GFAP) and aquaporin 4 (AQP4)^[18]. However, as what we show in the whole-mount retina fluorescent staining, RGCs were more susceptible to oxygen-glucose deprivation induced injury, with high mortality^[19]. Conversely, impaired neurocytes caused the release of proinflammatory cytokines and chemokines, and due to the breakdown of iBRB, they were diffused throughout the intraocular tissues, resulting in more extensive retinal capillaries degeneration^[5,20].

Although the protein sample we used in the Western blot came from whole retina which included not only ECs but also some pericytes, astrocytes, and so on, moesin is identified to express mainly in ECs, following immunohistochemical results also evidenced that both moesin and phospho-moesin were characteristically distributed in the retinal vascular endothelia, therefore it strengthens the endothelial specificity of moesin distribution in mice retina. ERM proteins comprising ezrin, radixin, and moesin, moesin links between the actin cytoskeleton and cell membrane, it is known as the dominant ERM molecule that tethers actin filaments. Moesin is masked in a quiescent state ordinarily, once phosphorylated, it is activated and functioned. Moesin has been investigated in

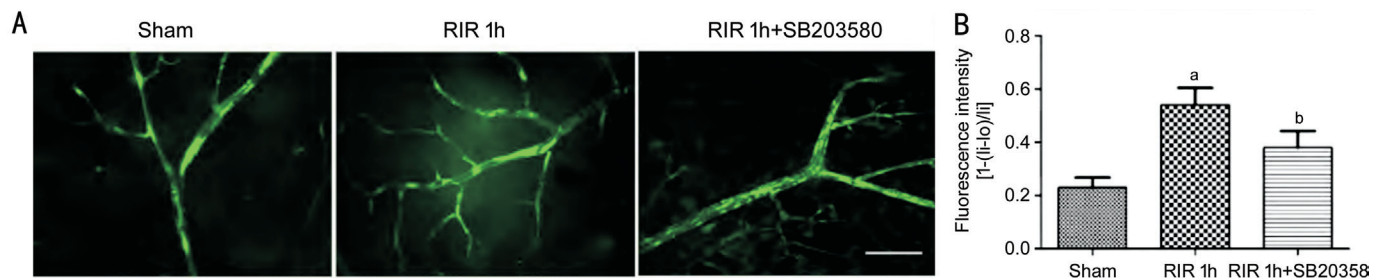


Figure 4 Effects of p38 inhibition with SB203580 in microvascular hyperpermeability induced by RIR insult A: Mice were treated with or without SB203580 intraperitoneally 30min prior to RIR treatment, followed by retina whole-mounted and exudation measurement 1h after reperfusion, pictures were captured under 400 \times magnification. B: Microvascular leakage was assessed as the relative dextran intensity outside the vessels to that inside the vessels. $n=5$. ^a $P<0.05$ vs Sham, ^b $P<0.05$ vs RIR 1h. Scale bar: 50 μ m.

several pathologies systemically, including cerebral circulation and lung injury^[21-22]. Here we firstly explored the involvement of retinal moesin phosphorylation in RIR related insults, a transient and time-dependent phosphorylation of moesin was detected, and the expression of phospho-moesin was peaked at 1h after reperfusion. It is consistent with previous study in HUVECs, both sphingosine-1-phosphate (S1P) and AGEs induced moesin phosphorylation in a time dependent manner^[8,23], indicating the requisite time point of moesin activation, regardless of the different cell types.

Inactive moesin reside in the cellular cortex area of cells, however provoked moesin are membrane-linked and bind with integral membrane proteins through its N-terminal FERM domain and with F-actin through their C termini, leading to cytoskeletal rearrangement and subsequent endothelial barrier dysfunction^[24]. Formation of actin stress fibers that induces EC contraction and increased permeability was once reported in influenza infected lung microvascular endothelium^[25]. Signaling mechanisms that mediates moesin activation and permeability alterations have been a subject of intense investigation. MAPKs represent the major signaling system that transduce a variety of extracellular signals, playing a vital role in different cellular responses to environmental stress^[26]. Guo *et al*^[8] specified p38 MAPK as the distinguishing subgroup of MAPKs by identifying for the effects of MAPKs on AGE-induced moesin phosphorylation with different inhibitors of the p38, ERK, and JNK pathways. Moreover, it was demonstrated that in human pulmonary ECs, depletion of p38 MAPK inhibits S1P-induced ERM phosphorylation^[27], hence we estimate that RIR-induced phosphorylation of moesin are mediated by p38 MAPK. Our present study showed that concomitantly with moesin activation, p38 MAPK were phosphorylated by RIR treatment, whereas preventing of p38 activation via inhibitor SB203580 not only downregulated the corresponding phosphorylation of p38, but also remarkably inhibited the phosphorylation of moesin and vascular hyperpermeability in RIR-insulted mouse retina.

However, it is noteworthy that the suppression of p38 MAPK only partially ameliorated the responses of moesin. It has been reported that other pathways like ROCK and PKC might also be involved in moesin phosphorylation^[25,28], thus inhibition of one pathway individually itself may not be sufficient to markedly attenuate the RIR induced moesin activation. What's more, ROCK may act upstream of p38 MAPK and PKC can mediate the activity of ROCK^[29-30], so it would be exciting to explore whether ROCK, PKC and other signal kinases also take part in RIR-insulted disruptions in endothelia, and furthermore the possible crosstalk between these pathways.

In conclusion, our study provides direct evidences *in vivo* to show that the up-regulation of moesin activity is involved in RIR induced retina endothelial dysfunction. P38 MAPK physically interacts with moesin and the RIR evoked phosphorylation of p38 causes moesin phosphorylation at threonine 558 residue. P38 MAPK-dependent moesin phosphorylation mediates RIR-triggered retina endothelial dysfunction. Our findings further emphasized the potential utility of a pharmacological target of the RIR-p38-moesin axis in retina iBRB disruption, though a moesin-knockout mice model would be more convincing to evidence moesin mediation, which we are continuing our efforts in conducting.

ACKNOWLEDGEMENTS

Authors' contributions: Xu J designed the study, performed the research, analysed data and wrote the paper. Liu Q performed the research and analyzed the data. Chen LJ wrote the paper. Ma M and Yu J helped design the study and checked the data. Xiong K and Wu J performed the research and analyzed the data.

Foundations: Supported by the Science and Technology Planning Project of Guangdong Province (No.201607010386); the Science and Technology Planning Project of Guangzhou (No.201504290959196).

Conflicts of Interest: Xu J, None; Liu Q, None; Ma M, None; Chen LJ, None; Yu J, None; Xiong K, None; Wu J, None.

REFERENCES

- 1 Country MW. Retinal metabolism: a comparative look at energetics in the retina. *Brain Res* 2017;1672:50-57.
- 2 Kohen MC, Tatlipinar S, Cumbul A, Uslu Ü. The effects of bevacizumab treatment in a rat model of retinal ischemia and perfusion injury. *Mol Vis* 2018;24:239-250.
- 3 Osborne NN, Casson RJ, Wood JP, Chidlow G, Graham M, Melena J. Retinal ischemia: mechanisms of damage and potential therapeutic strategies. *Prog Retin Eye Res* 2004;23(1):91-147.
- 4 Hartsock MJ, Cho H, Wu L, Chen WJ, Gong J, Duh EJ. A mouse model of retinal ischemia-reperfusion injury through elevation of intraocular pressure. *J Vis Exp* 2016(113).
- 5 Kaur C, Foulds WS, Ling EA. Blood-retinal barrier in hypoxic ischaemic conditions: basic concepts, clinical features and management. *Prog Retin Eye Res* 2008;27(6):622-647.
- 6 Wang Q, Fan A, Yuan Y, Chen L, Guo X, Huang X, Huang Q. Role of moesin in advanced glycation end products-induced angiogenesis of human umbilical vein endothelial cells. *Sci Rep* 2016;6:22749.
- 7 García-Ponce A, Citalán-Madrid AF, Velázquez-Avila M, Vargas-Robles H, Schnoor M. The role of actin-binding proteins in the control of endothelial barrier integrity. *Thromb Haemost* 2015;113(1):20-36.
- 8 Guo X, Wang L, Chen B, Li Q, Wang J, Zhao M, Wu W, Zhu P, Huang X, Huang Q. ERM protein moesin is phosphorylated by advanced glycation end products and modulates endothelial permeability. *Am J Physiol Heart Circ Physiol* 2009;297(1):H238-H246.
- 9 Wang J, Liu H, Chen B, Li Q, Huang X, Wang L, Guo X, Huang Q. RhoA/ROCK-dependent moesin phosphorylation regulates AGE-induced endothelial cellular response. *Cardiovasc Diabetol* 2012;11:7.
- 10 Dvorianchikova G, Degtarev A, Ivanov D. Retinal ganglion cell (RGC) programmed necrosis contributes to ischemia-reperfusion-induced retinal damage. *Exp Eye Res* 2014;123:1-7.
- 11 Dvorianchikova G, Barakat DJ, Hernandez E, Shestopalov VI, Ivanov D. Toll-like receptor 4 contributes to retinal ischemia/reperfusion injury. *Mol Vis* 2010;16:1907-1912.
- 12 Sellés-Navarro I, Villegas-Pérez MP, Salvador-Silva M, Ruiz-Gómez JM, Vidal-Sanz M. Retinal ganglion cell death after different transient periods of pressure-induced ischemia and survival intervals. A quantitative *in vivo* study. *Invest Ophthalmol Vis Sci* 1996;37(10):2002-2014.
- 13 Zhang W, Xu Q, Wu J, Zhou X, Weng J, Xu J, Wang W, Huang Q, Guo X. Role of Src in vascular hyperpermeability induced by advanced glycation end products. *Sci Rep* 2015;5:14090.
- 14 Inafuku S, Klokman G, Connor KM. The alternative complement system mediates cell death in retinal ischemia reperfusion injury. *Front Mol Neurosci* 2018;11:278.
- 15 Zheng L, Gong B, Hatala DA, Kern TS. Retinal ischemia and reperfusion causes capillary degeneration: similarities to diabetes. *Invest Ophthalmol Vis Sci* 2007;48(1):361-367.
- 16 Zhang W, Zhang Y, Guo X, Zeng Z, Wu J, Liu Y, He J, Wang R, Huang Q, Chen Z. Sirt1 protects endothelial cells against LPS-induced barrier dysfunction. *Oxid Med Cell Longev* 2017;2017:4082102.
- 17 Daruich A, Matet A, Moulin A, Kowalczyk L, Nicolas M, Sellam A, Rothschild PR, Omri S, Gélizé E, Jonet L, Delaunay K, de Kozak Y, Berdugo M, Zhao M, Crisanti P, Behar-Cohen F. Mechanisms of macular edema: Beyond the surface. *Prog Retin Eye Res* 2018;63:20-68.
- 18 Kaur C, Sivakumar V, Yong Z, Lu J, Foulds WS, Ling EA. Blood-retinal barrier disruption and ultrastructural changes in the hypoxic retina in adult rats: the beneficial effect of melatonin administration. *J Pathol* 2007;212(4):429-439.
- 19 Liu L, Jiang Y, Steinle JJ. Epac1 protects the retina against ischemia/reperfusion-induced neuronal and vascular damage. *PLoS One* 2018;13(9):e0204346.
- 20 Yoshida S, Yoshida A, Ishibashi T. Induction of IL-8, MCP-1, and bFGF by TNF-alpha in retinal glial cells: implications for retinal neovascularization during post-ischemic inflammation. *Graefes Arch Clin Exp Ophthalmol* 2004;42(5):409-413.
- 21 Kovacs-Kasa A, Gorshkov BA, Kim KM, Kumar S, Black SM, Fulton DJ, Dimitropoulou C, Catravas JD, Verin AD. The protective role of MLCP-mediated ERM dephosphorylation in endotoxin-induced lung injury *in vitro* and *in vivo*. *Sci Rep* 2016;6:39018.
- 22 Li Y, Li Q, Pan CS, *et al.* Bushen huoxue attenuates diabetes-induced cognitive impairment by improvement of cerebral microcirculation: involvement of RhoA/ROCK/moesin and src signaling pathways. *Front Physiol* 2018;9:527.
- 23 Xiao Y, Wu J, Yuan Y, Guo X, Chen B, Huang Q. Effect of moesin phosphorylation on high-dose sphingosine-1-phosphate-induced endothelial responses. *Mol Med Rep* 2018;17(1):1933-1939.
- 24 Bogatcheva NV, Zemskova MA, Gorshkov BA, Kim KM, Daglis GA, Poirier C, Verin AD. Ezrin, radixin, and moesin are phosphorylated in response to 2-methoxyestradiol and modulate endothelial hyperpermeability. *Am J Respir Cell Mol Biol* 2011;45(6):1185-1194.
- 25 Zhang C, Wu Y, Xuan Z, Zhang S, Wang X, Hao Y, Wu J, Zhang S. P38MAPK, Rho/ROCK and PKC pathways are involved in influenza-induced cytoskeletal rearrangement and hyperpermeability in PMVEC *via* phosphorylating ERM. *Virus Res* 2014;192:6-15.
- 26 Boutros T, Chevet E, Metrakos P. Mitogen-activated protein (MAP) kinase/MAP kinase phosphatase regulation: roles in cell growth, death, and cancer. *Pharmacol Rev* 2008;60(3):261-310.
- 27 Adyshev DM, Moldobaeva NK, Elangovan VR, Garcia JG, Dudek SM. Differential involvement of ezrin/radixin/moesin proteins in sphingosine 1-phosphate-induced human pulmonary endothelial cell barrier enhancement. *Cell Signal* 2011;23(12):2086-2096.
- 28 Adyshev DM, Dudek SM, Moldobaeva N, Kim KM, Ma SF, Kasa A, Garcia JGN, Verin AD. Ezrin/radixin/moesin proteins differentially regulate endothelial hyperpermeability after thrombin. *Am J Physiol - Lung Cell Mol Physiol* 2013;305(3):L240-L255.
- 29 Nwariaku FE, Rothenbach P, Liu Z, Zhu X, Turnage RH, Terada LS. Rho inhibition decreases TNF-induced endothelial MAPK activation and monolayer permeability. *J Appl Physiol* 2003;95(5):1889-1895.
- 30 Killock DJ, Ivetic A. The cytoplasmic domains of TNFalpha-converting enzyme (TACE/ADAM17) and L-selectin are regulated differently by p38 MAPK and PKC to promote ectodomain shedding. *Biochem J* 2010;428(2):293-304.